An alternate model for magnetization plateaus in the molecular magnet V_{15}

2001 J. Phys.: Condens. Matter 13 11717

(http://iopscience.iop.org/0953-8984/13/50/331)

INSTITUTE OF PHYSICS PUBLISHING JOURNAL OF PHYSICS: CONDENSED MATTER

J. Phys.: Condens. Matter **13** (2001) 11717–11725 PII: S0953-8984(01)27046-5

An alternate model for magnetization plateaus in the molecular magnet V_{15}

Indranil Rudra[1], **S Ramasesha**[1] **and Diptiman Sen**[2]

[1] Solid State and Structural Chemistry Unit, Indian Institute of Science, Bangalore 560012, India
[2] Centre for Theoretical Studies, Indian Institute of Science, Bangalore 560012, India

Received 23 July 2001, in final form 24 October 2001
Published 30 November 2001
Online at stacks.iop.org/JPhysCM/13/11717

Abstract

Starting from an antiferromagnetic Heisenberg Hamiltonian for the 15 spin-1/2 ions in V_{15}, we construct an effective spin Hamiltonian involving eight low-lying states (spin-1/2 and spin-3/2) coupled to a phonon bath. We numerically solve the time-dependent Schrödinger equation of this system, and obtain the magnetization as a function of temperature in a time-dependent magnetic field. The magnetization exhibits unusual patterns of hysteresis and plateaus as the field sweep rate and temperature are varied. The observed plateaus are not due to quantum tunnelling but are a result of thermal averaging. Our results are in good agreement with recent experimental observations.

The synthesis of high-nuclearity transition metal clusters such as Mn_{12}, Fe_8 and V_{15} [1] has provided an impetus to the study of magnetism on the nanoscale. These transition metal clusters are basically isolated transition metal complexes involving multi-dentate ligands; the chemical pathway between the metal ions in the transition metal complex dictates the nature of exchange interactions. The complex interplay of the topology of exchange interactions, magnetic dipolar interactions and spin–lattice coupling has yielded a rich physics on the nanoscale which includes quantum tunnelling, quantum phase interference and quantum coherence [2,3]. Quantum resonance tunnelling is characterized by the observation of discrete steps or plateaus in the magnetic hysteresis loops at low temperatures. The signature of quantum interference is seen in the variation of the tunnel splitting as a function of the azimuthal angle of the transverse field for tunnelling between $M_s = -10$ and $10 - n$ states in molecular magnets with ground state spin-10 [4]. Quantum coherence–decoherence studies are important from the stand point of application of these systems in quantum computations [5].

There have been several models proposed to understand these phenomena [6]. Quantum hysteresis and interference have largely been studied by using an effective spin Hamiltonian with dipolar interactions with a time varying external magnetic field. The time evolution of the states of the system are carried out within a master-equation approach [7]. The decoherence phenomena has been studied by using a simple two-state model in a transverse magnetic

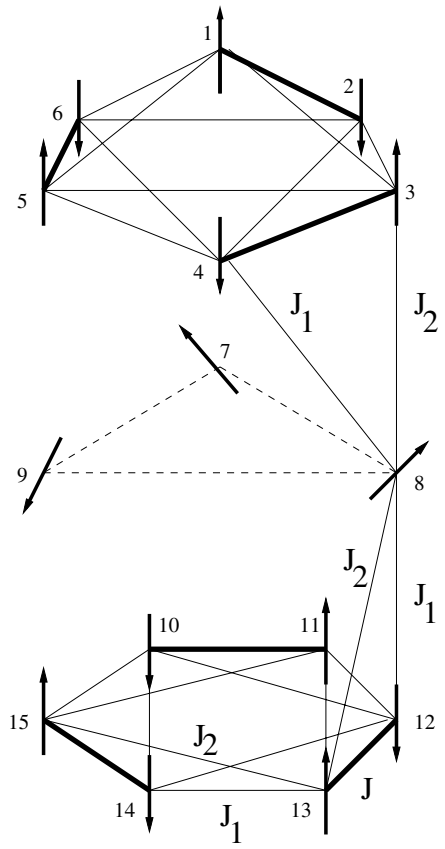

Figure 1. Schematic exchange interactions in a V_{15} cluster. There is no direct exchange interaction amongst the triangle spins. Interactions not shown explicitly can be generated from the C_3 symmetry of the system.

field [8]. Even though most of these clusters contain a fairly small number of metal ions, the spin on the metal ion, at least in the case of Fe_8 and Mn_{12}, is fairly large; a full quantum mechanical study of these systems is difficult because of the large Fock space dimensionalities of 1.69 and 100 million respectively. However, the V_{15} cluster is far more amenable to a rigorous quantum mechanical analysis because of the much smaller Fock space ($2^{15} \sim 33\,000$ dimensional) spanned by the unpaired spins of the system. A quantitative study of these systems requires at least the low-lying states of the full spin-Hamiltonian to be evolved in time quantum mechanically as the external magnetic field is ramped with time (as is done in experiments). In this paper, we study the magnetization of V_{15} by following its evolution as a function of a time-dependent magnetic field at different temperatures. The low-lying states are obtained by solving the exchange Hamiltonian corresponding to all the spins of the system. A spin–phonon interaction is then introduced in the Hamiltonian. We thermally average the magnetization over the low-lying states after each of these states is independently evolved. We find that this model reproduces most of the experimental features found in the magnetization studies of V_{15} [9], without invoking the concept of a 'phonon bottleneck'.

The schematic structure of V_{15} is shown in figure 1. Structural and related studies on the cluster indicate that within each hexagon, there are three alternating exchanges $J \approx 800$ K which are the strongest in the system, and they define the energy scale of the problem. Besides,

there are weaker exchange interactions between the spins involved in the strong exchange and also with the triangle spins which lie between the hexagons. All the exchange interactions are antiferromagnetic in nature. The exchange pathways and their strengths [9] are also shown in figure 1. What is significant in the cluster is the fact that the spins in the triangle do not experience direct exchange interactions of any significance. The exchange Hamiltonian of the cluster is solved using a valence bond basis in each of the total spin subspaces, for all the eigenvalues. It is found that two spin-1/2 states and a spin-3/2 state are split-off from the rest of the spectrum by a gap of 0.005 156 J [1]. These eight states almost exclusively correspond to the triangle spins and they are the only states which will make significant contributions to sub-Kelvin properties. We therefore set up an effective Hamiltonian in the Fock space of the three spins. We find that the lowest eight states of the exchange Hamiltonian of the full cluster is exactly reproduced by the following effective Hamiltonian

$$H_{sp-sp} = \epsilon I + \alpha(S_1 \cdot S_2 + S_2 \cdot S_3 + S_3 \cdot S_1) \tag{1}$$

where $\epsilon = -4.585\,9096$ and $\alpha = 0.003\,4373$ in units of the exchange J (see figure 1), reproduces the low-lying eigenstates to numerical accuracy. The first term in equation (1) denotes a constant shift in the energy levels of the three spins; this term plays no role in our calculations involving thermal averages.

The direct spin–spin interaction terms permitted by the C_3 symmetry are given by

$$H_{\mathrm{dip}} = \gamma[(S_+^3 + S_-^3) + \mathrm{i}(S_+^3 - S_-^3)]. \tag{2}$$

We have also introduced a coupling between the spin states of the cluster and the phonons. The spin–phonon interaction Hamiltonian which preserves the C_3 symmetry is phenomenologically given by [10]

$$H_{sp-ph} = q(b + b^\dagger)[(S_+^2 + S_-^2) + \mathrm{i}(S_+^2 - S_-^2) + (S_z^2 - \tfrac{1}{3}S^2)] \tag{3}$$

where q is the spin–phonon coupling constant, b ($b^\dagger$) is the phonon annihilation (creation) operator, and $\hbar\omega$ is the phonon frequency. For simplicity, we have assumed a single phonon mode although the molecule has various possible vibrational modes. The form of the interaction in equation (3) means that the phonons couple only to states with spin-3/2, because simple angular momentum considerations show that S_+^2, S_-^2 and $S_z^2 - S^2/3$ annihilate all the states with spin-1/2. Although the phonon space is infinite dimensional, we have restricted the dimensionality of the Fock space of the phonons to 15 considering the low temperatures of interest. That is, we do not consider states with more than 14 phonons; the vibrational quantum number j is restricted to a maximum value of 14.

The evolution of the magnetization as a function of the magnetic field has been studied by using the total Hamiltonian H_{total}, given by

$$H_{\mathrm{total}} = H_{sp-sp} + H_{\mathrm{dip}} + H_{sp-ph} + \hbar\omega(b^\dagger b + 1/2) + h_z(t)S_z + h_x(t)S_x \tag{4}$$

where we have assumed that besides an axial field $h_z(t)$, a small transverse field $h_x(t)$ could also be present to account for any mismatch between the crystalline z-axis and the molecular z-axis. The numerical method involves setting up the Hamiltonian matrix in the product basis of the spin and phonon states $|i, j\rangle$, where $|i\rangle$ corresponds to one of the eight spin configurations of the three spins, and j varies from 0 to 14, corresponding to the 15 phonon states retained in the problem. The values we have assigned to the different parameters are $\gamma = 10^{-3}$, $q = 10^{-4}$ and $\hbar\omega = 1.25 \times 10^{-4}$, all in units of the exchange J (see figure 1). In figure 2, we show the energy level ordering of the effective spin Hamiltonian and the effect of the magnetic field on the eigenvalue spectrum. We also show the couplings between various states brought about by the magnetic dipolar terms and the spin–phonon terms; note that the spin-1/2 and spin-3/2 states are not connected to each other by these terms.

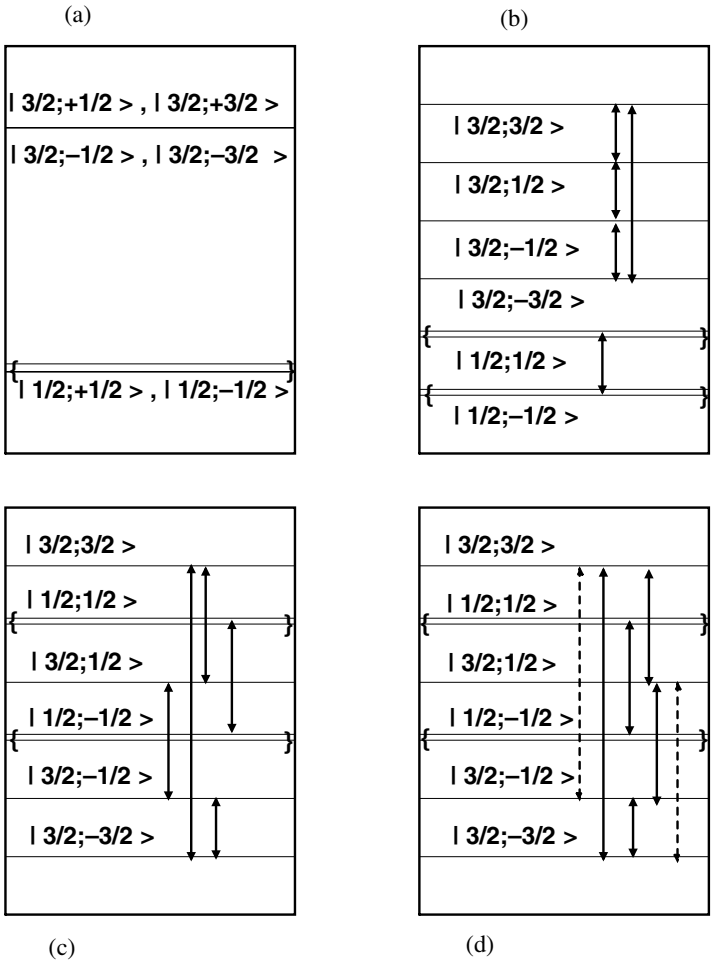

Figure 2. (a) Eigenstates of the effective spin Hamiltonian H_{sp-sp}, (b) eigenstates in the presence of a moderate axial field. Arrows show the states connected by the dipolar terms and the transverse field, (c) is the same as (b) but in a stronger field, (d) describes the effect of spin–phonon terms (shown by arrows with broken lines) on (c).

To study the magnetization phenomena, we start with the direct product eigenstates of H_{sp-sp} and $\hbar\omega(b^{\dagger}b + 1/2)$, and independently evolve each of the 120 states ψ_{ij} by using the time evolution operator

$$\psi(t + \Delta t) = \mathrm{e}^{-\mathrm{i}H_{\mathrm{total}}\Delta t/\hbar}\psi(t). \tag{5}$$

The evolution is carried out in small time steps by applying the evolution operator to the state arrived at in the previous step. The magnetic field is changed step-wise in units of 0.015 T. At each value of the magnetic field, the system is allowed to evolve for 300 time steps of size Δt, before the field is changed to the next value. At every time step, the average magnetization $\langle M(t)\rangle$ is calculated as

$$\langle M(t)\rangle = \sum_{i=1}^{8}\sum_{j=0}^{14}\frac{\mathrm{e}^{-\beta[w_i+h_z(t)m_i]}}{Z_{\mathrm{spin}}}\frac{\mathrm{e}^{-\beta\hbar\omega(j+1/2)}}{Z_{ph}}\langle\psi_{ij}(t)|\hat{S}_z|\psi_{ij}(t)\rangle \tag{6}$$

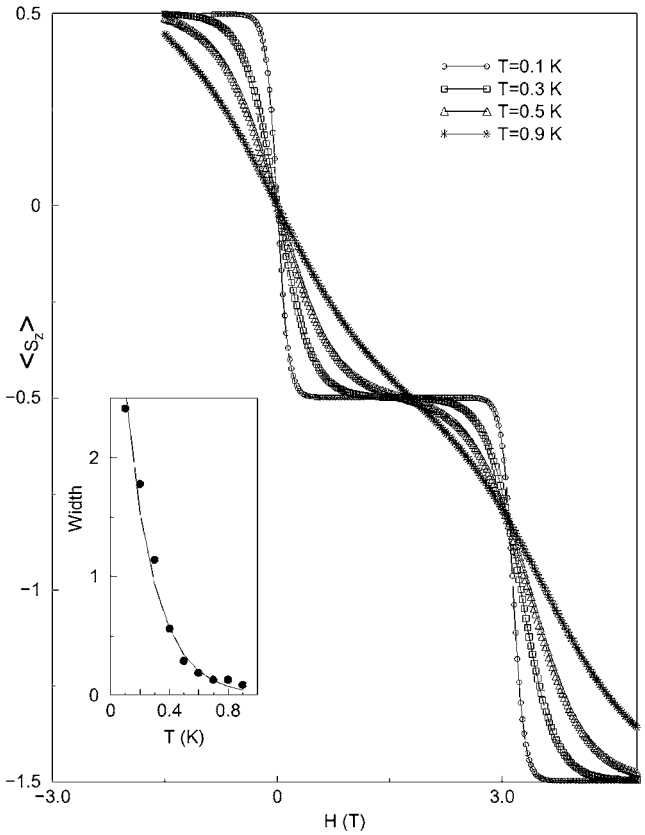

Figure 3. Plot of magnetization versus axial field at different temperatures. Inset shows plateau width as a function of temperature (full circles) falling off exponentially.

where w_i and m_i are the eigenvalues and magnetizations of eigenstates of H_{sp-sp}, $\beta = 1/k_{\rm B}T$, Z_{ph} is the phonon partition function of $\hbar\omega(b^{\dagger}b + 1/2)$, and $Z_{\rm spin}$ is the partition function of H_{sp-sp} in the presence of the axial magnetic field. Implicit in equation (6) is the important assumption that at each value of the magnetic field, the system has sufficient time to reach thermal equilibrium. The value of $\langle M(t)\rangle$ obtained by this method is approximately equal to that obtained from a density matrix technique if the dipolar and spin–phonon coupling constants γ and q are small, so that for each state $|\psi_{ij}\rangle$, the eigenvalue of the total Hamiltonian $\hat{H}_{\rm tot}$, in a magnetic field $h_z(t)$ at any instant t, is close to the value of $(w_i + m_i h_z(t) + (j + 1/2)\hbar\omega)$ that we have used in the Boltzmann weight in equation (6).

In figure 3, we show the magnetization plots of the system for different temperatures. We see that at low temperatures, the plateaus are very pronounced. The plateau width at $\langle S_z\rangle = -0.5$ corresponds to 2.8 T at $T = 0.1$ K which is in good agreement with the experimental value [9] assuming that $J = 800$ K. The literature [1, 9] estimates of the exchange constants do not reproduce the experimental value of the field (2.82 T) at which the magnetization jumps from $\langle S_z\rangle = -0.5$ to $\langle S_z\rangle = -1.5$. In figure 4, we have magnified the region of the magnetic field at which this jump occurs for the three sets of values of the exchange parameters. The sharpness of the transitions however is comparable in all the three cases.

Furthermore, we find that the plateau has vanished at a temperature of 0.9 K which is also in agreement with the experimental value [9]. The plateau width is maximum at $T = 0$

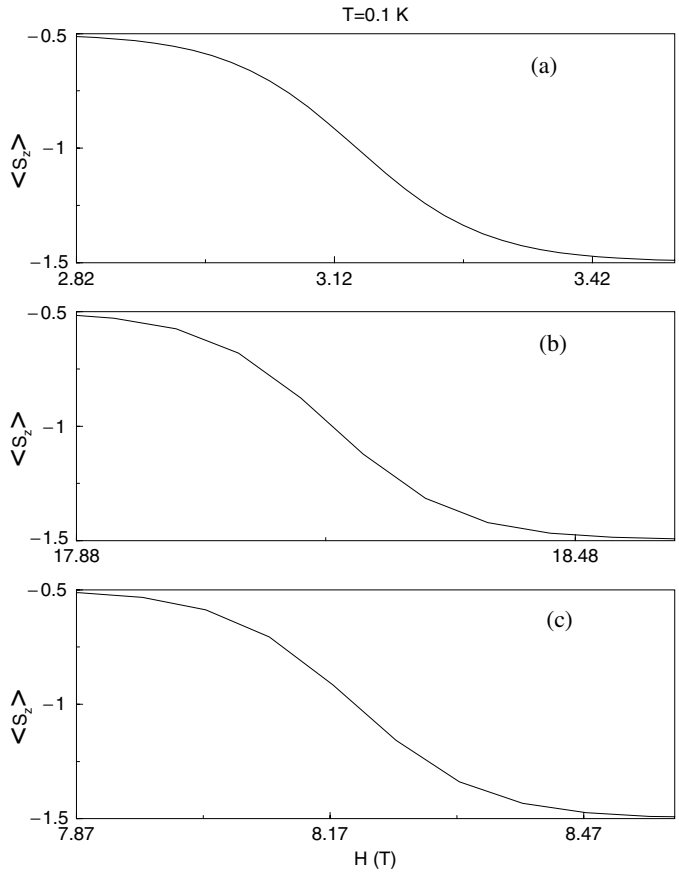

Figure 4. Magnetization versus magnetic field at $T = 0.1$ K in the neighbourhood of the transition from $\langle S_z \rangle = -0.5$ to -1.5 for (a) $J = 800$ K, $J_1 = 54$ K, $J_2 = 160$ K, (b) $J = 800$ K, $J_1 = 150$ K, $J_2 = 300$ K [9], and (c) $J = 756$ K, $J_1 = 29$ K, $J_2 = 179$ K [1].

since thermal excitations cannot occur at that temperature. The inset of figure 3 shows the temperature variation of the plateau width. We note that the plateau width falls off rapidly with temperature, and an exponential fit to $W = A \exp(-T/\Omega)$ gives the characteristic temperature Ω to be 0.2 K, with $A = 0.0070$. This small value of Ω is because there are no large barriers between the different magnetization states in this system, unlike the high spin molecular magnets such as Mn_{12} [6].

Note that the jumps in the magnetization $\langle S_z \rangle$ in figure 3 occur at the field values $0T$ and $3T$; this is because at those field values, several spin states are degenerate. At $H \sim 0T$, the ground state is four-fold degenerate corresponding to two spin-1/2 states with $S_z = \pm 1/2$. A finite magnetic field breaks the $S_z = \pm 1/2$ degeneracy. At $T = 0$, a state with only one spin orientation is occupied, resulting in a jump in magnetization. At $H \sim 3T$, the $S_z = -3/2$ state crosses the $S_z = -1/2$ states leading to a second jump in the magnetization at that magnetic field.

We also observe that when the field is swept more rapidly, there are additional plateaus at intermediate values of magnetization. For example, in figure 5 the field sweep rate is increased by a factor of five compared to figure 3, and we find a small plateau of width $0.03T$ near $H = 0.15T$ at a value of $\langle S_z \rangle = -0.375$. This is because near that field, some of the

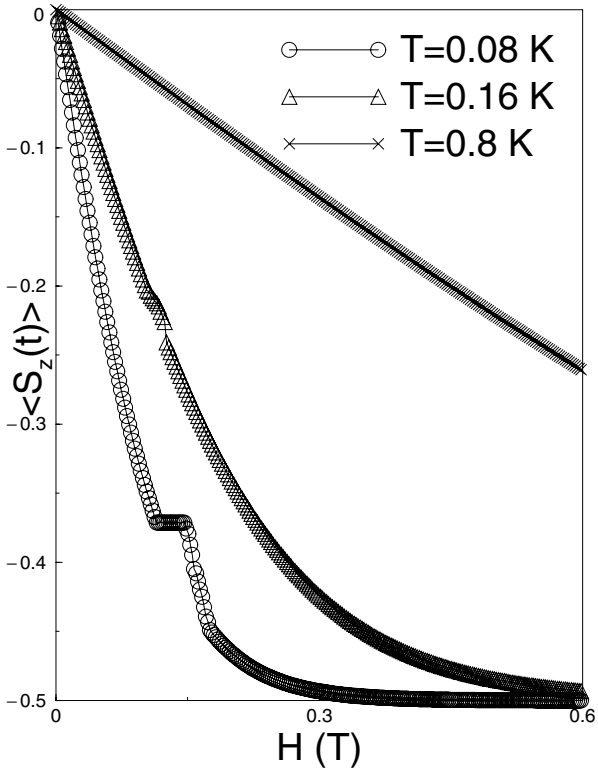

Figure 5. Magnetization as a function of axial field for a faster sweep rate at three different temperatures.

spin-3/2 states become degenerate in energy; subsequently, as the magnetic field is increased, the system stays locked in some of those states if the sweep rate is too high. This plateau vanishes on warming the system slightly.

We have also studied the effect of cycling the magnetic field. In figure 6, we show the magnetization as a function of the field at different temperatures and sweep rates. It is interesting to see that the system does not have either remnance or coercivity; all the hysteresis plots pass through the origin. The effect of varying the rate of scanning the field is also shown in figure 6. We find that as the scanning rate increases, the hysteresis in the plot of magnetization versus field decreases, and the plateau feature is almost identical in both the scanning directions. This could be because of the slow relaxation of the magnetization which is indeed the reason why the plateaus occur in the first place. We also find that the transverse field term does not affect any of our results significantly.

To summarize, we have derived an effective Hamiltonian from the exchange Hamiltonian of the full V_{15} system. In the presence of a time varying magnetic field, the states of the effective Hamiltonian are allowed to evolve under the influence of magnetic dipolar interactions and a spin–phonon coupling. During the time evolution, the magnetization is followed as a function of the applied magnetic field. The calculated M versus H plots show magnetization plateaus at low temperatures. The width of the plateau at low temperature as well as the temperature at which the plateau vanishes are in excellent agreement with experimental values. It is also shown that the number of plateaus observed depends upon the scanning speed of the magnetic field. When the magnetic field is cycled, the hysteresis plots pass through the origin

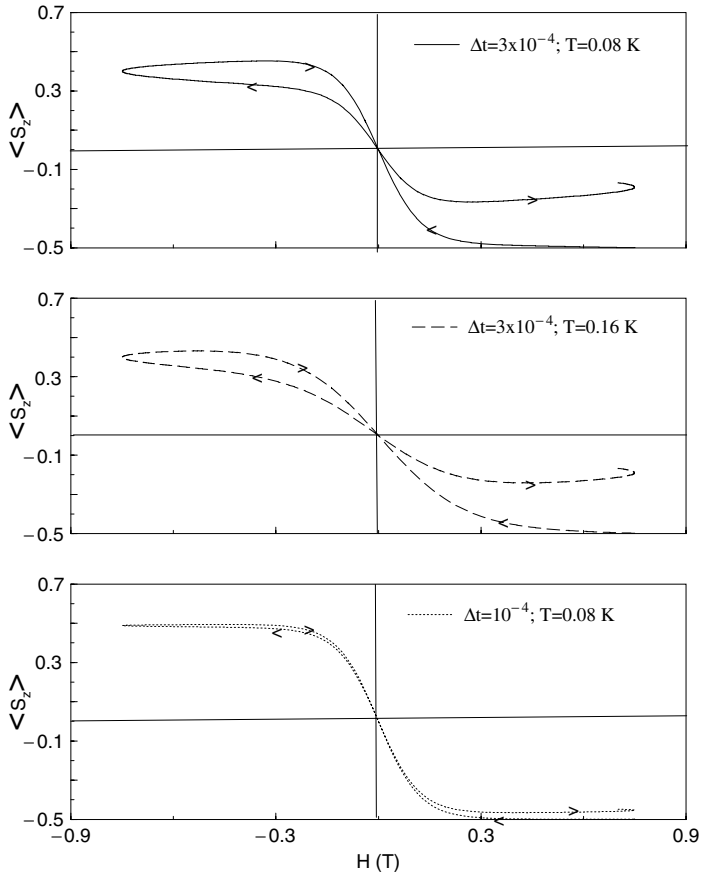

Figure 6. Magnetization versus axial field for a full cycling of the field at different temperatures and sweep rates.

indicating the absence of remnance and coercion. The hysteresis is pronounced for slow scanning speeds. From our results, it appears that the magnetization plateaus in V_{15} is not a consequence of quantum resonant tunnelling but is a result of thermal averaging. We also find that the magnetization does not show any oscillation with time during evolution indicating the absence of quantum tunnelling.

Acknowledgment

We thank the Council of Scientific and Industrial Research, India for their grant no 01(1595)/99/EMR-II.

References

[1] Lis T 1980 *Acta Crystallogr.* B **36** 2042
Delfas C, Gatteschi D, Pardi L, Sessoli R, Wieghardt K and Hanke D 1993 *Inorg. Chem.* **32** 3099
Barra A L, Gatteschi D, Pardi L, Müller A and Döring J 1992 *J. Am. Chem. Soc.* **114** 8509

[2] Gunther L and Barbara B (ed) 1995 *Quantum Tunneling of Magnetization—QTM'94 (NATO ASI Series E vol 301)* (Dordrecht: Kluwer)
Friedman J R, Sarachik M P, Tejada J and Ziolo R 1996 *Phys. Rev. Lett.* **76** 3830

Thomas L, Lionti F, Ballou R, Gatteschi D, Sessoli R and Barbara B 1996 *Nature* **383** 145 and references therein
[3] Gatteschi D, Pardi L, Pardi A L, Müller A and Döring J 1991 *Nature* **354** 465
[4] Wernsdorfer W and Sessoli R 1999 *Science* **284** 133
[5] Chudnovsky E M 1996 *Science* **274** 938
Stamp P C E 1996 *Nature* **383** 125
Thomas L, Lionti F, Ballou R, Gatteschi D, Sessoli R and Barbara B 1996 *Nature* **383** 145
[6] De Raedt H, Miyashita S, Saito K, Garcia-Pablos D and Garcia N 1997 *Phys. Rev.* B **56** 11 761
Garanin D A and Chudnovsky E M 1997 *Phys. Rev.* B **56** 11 102
Garg A 1998 *Phys. Rev. Lett.* **81** 1513
Tupitsyn I S 1998 *JETP Lett.* **67** 32
(Tupitsyn I S 1997 *Preprint* cond-mat/9712302)
Prokofev N V and Stamp P C E 1996 *J. Low. Temp. Phys.* **104** 143
Katsnelson M I, Dobrovitski V V and Harmon B N 1999 *Phys. Rev.* B **59** 6919
Rudra I, Ramasesha S and Sen D 2001 *Phys. Rev.* B **64** 014408
[7] Politi P, Rettori A, Hartmann-Boutron F and Villain J 1995 *Phys. Rev. Lett.* **75** 537
Fort A, Rettori A, Villain J, Gatteschi D and Sessoli R 1998 *Phys. Rev. Lett.* **80** 612
[8] Dobrovitski V V, Katsnelson M I and Harmon B N 2000 *Phys. Rev. Lett.* **84** 3458
[9] Chiorescu I, Wernsdorfer W, Müller A, Bögge H and Barbara B 2000 *Phys. Rev. Lett.* **84** 3454
Chiorescu I, Wernsdorfer W, Müller A, Bögge H and Barbara B 2000 *J. Magn. Magn. Mater.* **221** 103
[10] Leuenberger M N and Loss D 1999 *Europhys. Lett.* **46** 692
Leuenberger M N and Loss D 2000 *Phys. Rev.* B **61** 1286
Callen E and Callen H B 1965 *Phys. Rev.* A **139** 455